

# HMXB, ULX and star formation

M.Gilfanov<sup>ab</sup>, H.-J.Grimm<sup>a</sup> and R.Sunyaev<sup>ab</sup>

<sup>a</sup>Max-Planck-Institut für Astrophysik, 85741 Garching b.München, Germany

<sup>b</sup>Space Research Institute, Profsoyuznaya 84/32, Moscow, Russia

Based on recent X-ray observations of the Milky Way, Magellanic Clouds and nearby starburst galaxies we study population of high mass X-ray binaries, their connection with ultra-luminous X-ray sources and relation to the star formation. Although more subtle SFR dependent effects are likely to exist, the data in the  $\lg(L_X) \sim 36 - 40.5$  luminosity range are broadly consistent with existence of a “universal” luminosity function of HMXBs, which can be roughly described as a power law with differential slope of  $\sim 1.6$  and a cutoff at  $\lg(L_X) \sim 40.5$ . The ULX sources found in many starburst galaxies occupy the high luminosity end of this single slope power law distribution, whereas its low luminosity part is composed of “ordinary” high mass X-ray binaries, observed, e.g. in the Milky Way and Magellanic Clouds.

As the normalization of the “universal” luminosity function is proportional to the star formation rate, the number and/or the collective X-ray luminosity of HMXBs can be used to measure the current value of SFR in the host galaxy. Distant (unresolved) starburst galaxies observed by Chandra at redshifts of  $z \sim 0.2 - 1.3$  obey the same  $L_X$ –SFR relation as local galaxies, indicating that the ULXs at these redshifts were not significantly more luminous than those found in nearby galaxies.

## 1. INTRODUCTION

An unusual class of compact sources – ultra-luminous X-ray sources, has been discovered in nearby galaxies more than a decade ago [2,3]. Although bright,  $L_X > 10^{39}$  erg/s, point-like sources are found both in young star forming galaxies and in old stellar population of elliptical galaxies, the most luminous and exotic objects are associated with actively starforming galaxies. Their nature and relation to more ordinary X-ray binaries is still a matter of a significant debate. Based on a simple Eddington luminosity argument, they appear to be powered by accretion onto an intermediate mass object – a black hole with the mass in the hundreds-thousands solar masses range. However, a number of alternative models have been considered as well – from collimated radiation to  $\sim$ stellar mass black holes, representing the high mass tail of the standard stellar evolution sequence and accreting in the near- or slightly super-Eddington regime.

Sub-arcsec angular resolution of Chandra observatory opened a new era in studying population of compact sources in nearby galaxies. For

the first time an opportunity was presented to observe compact sources in a nearly confusion free regime and to investigate their relation to fundamental parameters of the host galaxy, such as its stellar mass and star formation rate. Depending on the mass of the optical companion, X-ray binaries are subdivided in to two classes – low and high mass X-ray binaries, having significantly different evolutionary time scale,  $\sim 10^{6-7}$  and  $\sim 10^{9-10}$  years respectively [12]. The prompt emission from HMXBs makes them a potentially good tracer of the very recent star formation activity in the host galaxy [11]. The LMXBs, on the other hand, have no relation to the present star formation, but, rather, are related to the stellar content of the host galaxy [4]. Chandra observations of the nearby galaxies present a possibility to verify this simple picture and to calibrate the relation between the HMXB population and the current value of SFR. This opens a new way to determine the star formation rate in relatively closeby galaxies as well as in young and very distant ones. Detailed study of the population of the compact sources in star forming galaxies can also shed the light on the mystery of the ULXs.

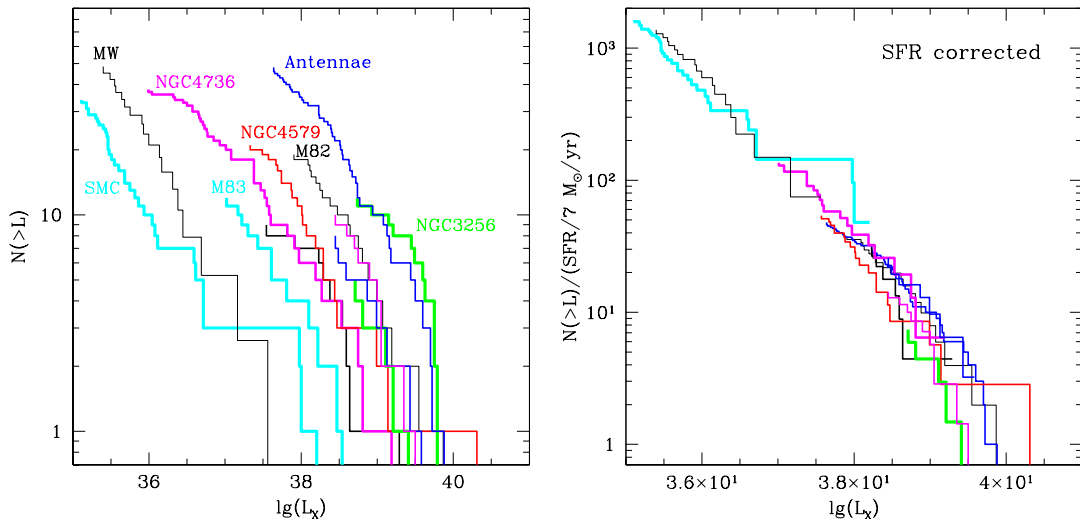


Figure 1. *Left:* The luminosity functions of compact X-ray sources in nearby galaxies obtained by Chandra. *Right:* The luminosity functions for the same galaxies scaled by the ratio of their star formation rate to that of Antennae.

## 2. “UNIVERSAL” LUMINOSITY FUNCTION OF HMXBs

In order to study the HMXB population and its relation to star formation we selected a number of nearby late type galaxies observed by Chandra, based primarily on two criteria. (i) The galaxy can be spatially resolved by Chandra, so that the contribution of a central AGN can be discriminated and the luminosity functions of the compact sources can be constructed without severe confusion effects. (ii) The galaxy has sufficiently high SFR/mass ratio, to ensure that the population of X-ray binaries is dominated by HMXBs and the LMXB contribution can be safely ignored [5]. For the Milky Way we explicitly selected HMXBs, based on results of [7]. For each galaxy, the star formation rate was determined combining the results from conventional SFR indicators, [9] (FIR, UV,  $H_\alpha$  and radio). The SFR values in the sample range from  $\sim 0.15$  to  $\sim 7 M_\odot/\text{yr}$ . Further details and references to the X-ray data are given in [8].

The Fig.1 (left panel) shows observed luminos-

ity functions. They are characterized by a large spread in the number of sources and in the luminosity of the brightest source. However, after being rescaled to the same value of the star formation rate, they appear to match each other both in the slope of the distribution and the normalization (right panel in Fig.1). Although a finite dispersion might still exist, especially at the high luminosity end, the rescaled luminosity functions occupy a rather narrow band in the  $N-L_X$  plane, despite of large dynamical range of the star formation rates, a factor of  $\sim 50$ . We further combine the data for five nearby starburst galaxies with the best known luminosity functions, having cumulative star formation rate of  $\approx 16 M_\odot/\text{yr}$ , and compare them with the luminosity distributions of two low SFR galaxies, the Milky Way and SMC (Fig.2). As previously, a good agreement both in the slope and normalization of luminosity distributions is obvious. The fit to combined data with a power law distribution gives the slope of  $\alpha \approx 1.6$ , a cut-off at  $L_{\text{cut}} \approx (2-3) \cdot 10^{40}$  erg/s and the normalization proportional to the star

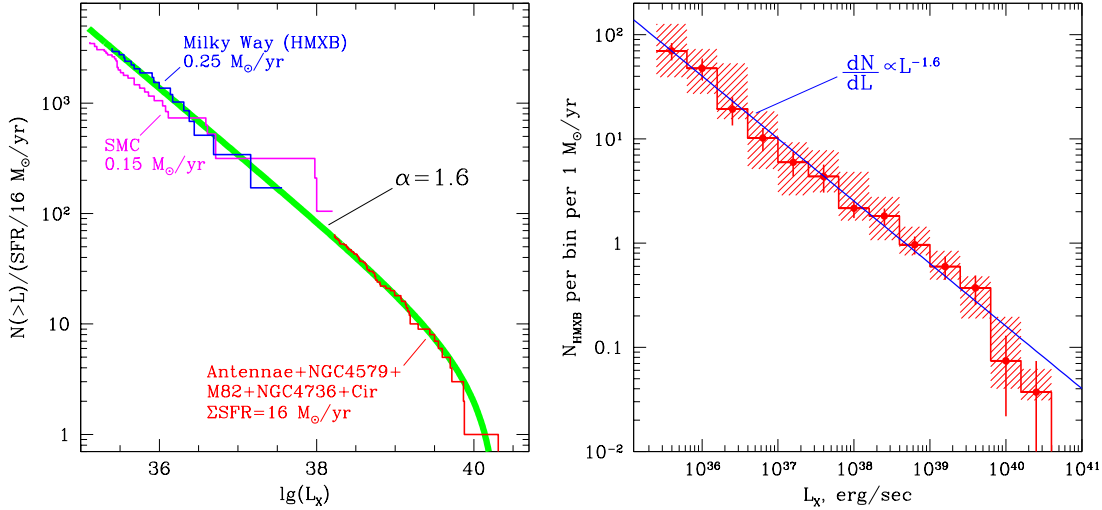


Figure 2. *Left*: Combined luminosity function of compact X-ray sources in starburst galaxies and the luminosity functions of HMXBs in the Milky Way and SMC. The thick grey line is the best fit to the starburst galaxies, Eq.(1). *Right*: Average differential luminosity function of the galaxies from our Chandra sample. The straight line is a power law defined by eq.(1). The shaded area illustrates the amplitude of systematic errors (90% confidence level) associated with uncertainties in the adopted SFR values (assuming 30% relative error) and the distances (20% relative error).

formation rate:

$$\frac{dN}{dL} = (3.3^{+1.1}_{-0.8}) \cdot SFR \cdot L_{38}^{-1.61 \pm 0.12} \quad (1)$$

where SFR is formation rate for massive stars,  $M > 5M_{\odot}$ . Within the accuracy of the present analysis, this can be regarded as a “universal” luminosity function of high mass X-ray binaries in nearby star forming galaxies. The Fig.2 shows the average differential luminosity function of HMXBs obtained using the data of all galaxies from our Chandra sample.

### 3. HIGH MASS X-RAY BINARIES AS A STAR FORMATION INDICATOR

As the population of high mass X-ray binaries (i.e. the normalization of the luminosity function and the number of sources) is proportional to SFR, eq.(1), they can be exploited to measure star formation rate in the host galaxy. Such a

method, based on the X-ray emission of a galaxy, might circumvent one the main sources of uncertainty of conventional SFR indicators – absorption by dust and gas [9]. Indeed, galaxies are mostly transparent to X-rays above  $\sim 2$  keV, except for the densest parts of the most massive molecular clouds.

For nearby, spatially resolved galaxies, the star formation rate can be determined via a direct fitting of the luminosity distribution of the compact sources or counting the number of sources above a given luminosity threshold. For distant, unresolved galaxies one can use the total luminosity of the galaxy.

There are, however, two main complicating factors in using the X-ray luminosity of a galaxy as a SFR indicator: (i) X-ray emission from the central supermassive black hole, which even in the case of a low luminosity AGN can easily outshine X-ray binaries. This does not present a

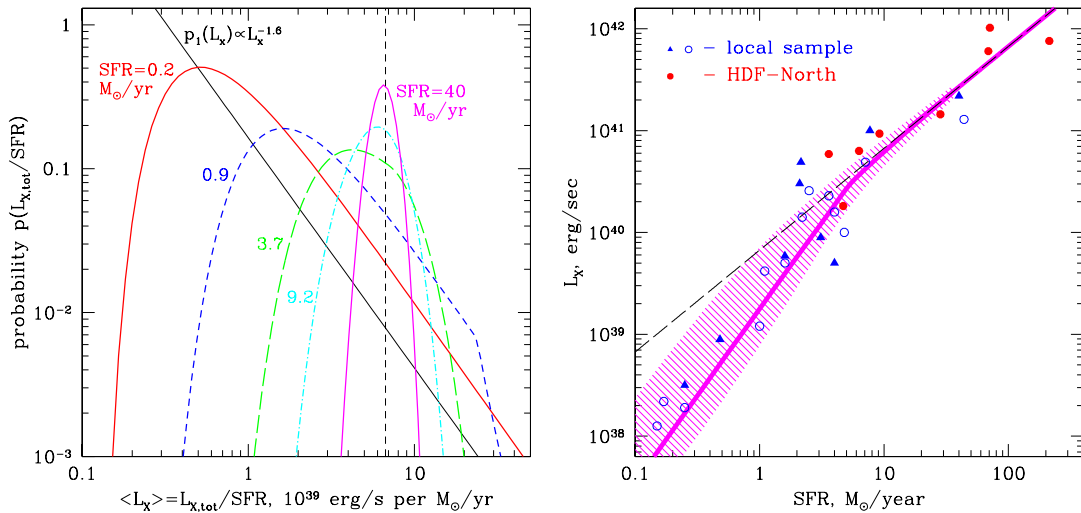


Figure 3. *Left:* The probability distributions  $p(L_{\text{tot}}/SFR)$  for different values of SFR. The vertical dashed line shows the expectation mean, defined by eq.(2). *Right:* The  $L_X$ –SFR relation. The open circles are nearby galaxies observed by Chandra, the filled triangles are nearby galaxy observed by ASCA and BeppoSAX, for which only total luminosity is available, the filled circles are distant star forming galaxies from the Hubble Deep Field North. The thick grey line is relation between the star formation rate and the most probable value of the total luminosity, predicted from the “universal” luminosity function of HMXBs, the shaded area shows 67% intrinsic spread of the  $L_X$ –SFR relation, the dashed line is the expectation mean, defined by eq.(2).

problem in nearby ( $D < 20 - 30$  Mpc) galaxies as the Chandra resolution is sufficient to separate contribution of the central source, but might become an important source of contamination in spatially unresolved galaxies. (ii) Contribution of low mass X-ray binaries. This equally affects nearby and distant galaxies, as LMXBs can not be easily separated from HMXBs using the X-ray data in the Chandra bandpass, and the optical identifications are (potentially) available for the most nearby galaxies only. However, as the LMXB population scales linearly with the stellar mass of the host galaxy [4], their contribution can be estimated and, potentially, corrected for. Obviously, at sufficiently high values of  $SFR/M_*$  it can be safely neglected, [5].

To further calibrate the  $L_X$ –SFR relation and verify its applicability to distant galaxies, we ex-

tended our sample to include the spatially unresolved galaxies observed by ASCA and BeppoSAX and distant star forming galaxies detected by Chandra in the Hubble Deep Field North [1] (see [8] for details and references). As for the galaxies from our spatially resolved Chandra sample, star formation rates were determined by the conventional, non X-ray methods. The combined data are shown in the  $L_X$ –SFR plane in Fig.3.

### 3.1. Effects of statistics and $L_X$ –SFR relation

A seemingly obvious expression for the total luminosity can be obtained integrating the luminosity distribution (1):

$$\langle L_{\text{tot}} \rangle = \int_{L_{\text{min}}}^{L_{\text{cut}}} \frac{dN}{dL} L dL \propto SFR \quad (2)$$

implying, that the total luminosity is proportional to the star formation rate. We note, however, that the quantity of interest is a sum of the luminosities of discrete sources:

$$L_{\text{tot}} = \sum_k L_k \quad (3)$$

with  $L_k$  obeying a power law probability distribution given by eq.(1). For a sufficiently flat slope,  $\alpha < 2$ , the total luminosity  $L_{\text{tot}}$  will be defined by the brightest sources, corresponding to the high luminosity end of the power law distribution eq.(1). Their actual number in a galaxy will obey the Poisson distribution  $P(n, \mu) = \mu^n e^{-\mu} / n!$  (with  $\mu \propto \text{SFR}$ ), which for small values of  $\mu$  is significantly asymmetric. As a consequence, for a galaxy with small SFR, the probability distribution  $p(L_{\text{tot}})$  will be also strongly asymmetric, as illustrated by the left panel in Fig.3. Because of its skewness, the mode of the  $p(L_{\text{tot}})$  distribution – the value of  $L_{\text{tot}}$  that would be most likely measured in an arbitrarily chosen galaxy, is not equal to the expectation mean defined by eq.(2). Only in the large SFR limit, when there are sufficiently many sources with luminosities  $L \sim L_{\text{cut}}$ , these two quantities become close to each other.<sup>1</sup>

The difference between these two quantities is further illustrated in the right panel in Fig.3, showing the predicted  $L_X$ –SFR relation, calculated using the parameters of the “universal” HMXB luminosity function, eq.(1). The solid line in the figure shows the SFR–dependence of the mode of the probability distribution  $p(L_{\text{tot}})$  and predicts the *most probable* value of the X-ray luminosity of a randomly chosen galaxy. If observations of many (different) galaxies with close values of SFR are performed, the obtained values of  $L_{\text{tot}}$  will obey the probability distribution depicted in the left panel of Fig.3. The average of the measured values of  $L_{\text{tot}}$  will be equal to the expectation mean given by eq.(2) and shown by the dashed straight lines in the left and right panels of Fig.3. Due to the properties of the probability distribution  $p(L_{\text{tot}})$  these two quantities are not identical in the low SFR limit, when the total lu-

minosity is defined by a small number of the most luminous sources.

### 3.2. $L_X$ –SFR relation: predicted vs. observed

The right panel in Fig.3 compares the data with the predicted  $L_X$ –SFR relation. Good agreement, both in the non-linear low SFR regime and at high SFR values is apparent. The relations between total X-ray luminosity of a galaxy due to HMXBs and the star formation rate are:

$$\text{SFR}[\text{M}_{\odot}/\text{yr}] \approx \frac{L_{2-10 \text{ keV}}}{6.7 \cdot 10^{39} \text{ erg/s}} \quad (4)$$

in the linear regime and

$$\text{SFR}[\text{M}_{\odot}\text{yr}^{-1}] \approx \left( \frac{L_{2-10 \text{ keV}}}{2.6 \cdot 10^{39} \text{ erg/s}} \right)^{0.6} \quad (5)$$

in the non-linear regime, corresponding to  $\text{SFR} < 4.1 \text{ M}_{\odot} \text{ yr}^{-1}$  ( $L_{2-10 \text{ keV}} < 2.8 \cdot 10^{40} \text{ erg s}^{-1}$ ). The former, linear, regime of the  $L_X$ –SFR relation was studied independently by [10] based on ASCA and BeppoSAX data. Note that their equation (12) agrees with our eq.(4) within  $\sim 30$  per cent.

Due to skewness of the probability distribution  $p(L_{\text{tot}})$ , large and asymmetric dispersion around the solid curve in Fig.3 is expected in the non-linear low SFR regime. This asymmetry is already seen from the distribution of the points in Fig.3 – at low SFR values there are more points above the solid curve, than below. Moreover, the galaxies lying significantly above the solid and dashed curves in Fig.3 should be expected at low SFR and will inevitably appear as the plot is populated with more objects. Such behavior differs from a typical astrophysical situation and should not be ignored when analyzing and fitting the  $L_X$ –SFR relation in the low SFR regime. In particular, the standard data analysis techniques – least square and  $\chi^2$  fitting become inadequate.

## 4. DISCUSSION

### 4.1. High luminosity cut-off in the HMXB luminosity function

The existence of the linear regime in the  $L_X$ –SFR relation is a direct consequence of the cut-off in the luminosity function. The position of

<sup>1</sup>Obviously in the case of e.g. flat ( $dN/dL = \text{const}$ ) or Gaussian flux distribution the most probable value of  $L_{\text{tot}}$  always equals to the expectation mean defined by eq.(2).

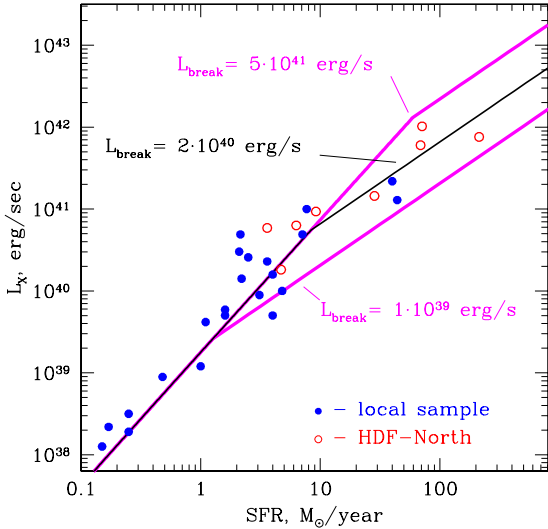


Figure 4. Dependence of the  $L_X$ –SFR relation on the maximum luminosity of the sources,  $L_{\text{cut}}$ . The three curves, corresponding to different values of  $L_{\text{cut}}$  coincide in the non-linear low SFR regime but differ in the position of the break between linear and non-linear regimes. The data are the same as in Fig.3.

the break between non-linear and linear parts of the  $L_X$ –SFR relation depends on the slope of the luminosity function and the value of the cut-off luminosity (Fig.4):  $\text{SFR}_{\text{break}} \propto L_{\text{cut}}^{\alpha-1}$ . This allows one to constrain parameters of the luminosity distribution of compact sources using the data of spatially unresolved galaxies.

Agreement of the predicted  $L_X$ –SFR relation with the data both in high and low SFR regimes gives an independent confirmation of the existence of a cut-off in the luminosity function of HMXBs at  $L_{\text{cut}} \sim \text{several} \times 10^{40}$  erg/s (Fig.3,4). It also confirms that  $L_X$ –SFR data, including the high redshift galaxies from Hubble Deep Field North, are consistent with the HMXB luminosity function parameters, derived from significantly fewer galaxies, than plotted in Figs.3,4.

## 4.2. Ultraluminous X-ray sources

One of the surprising results of this study is a smooth, single slope power law shape of the average luminosity function of compact sources in star forming galaxies, without any significant steps and features in a broad luminosity range,  $\lg(L_X) \sim 36 - 40.5$  (Fig.2). The high luminosity end,  $\lg(L_X) > 39$ , of this distribution corresponds to ultraluminous X-ray sources. Its low luminosity end, on the other hand, is composed of ordinary X-ray binaries, powered by accretion onto a  $\sim$ stellar mass compact objects. This result constrains the range of possible models for ULXs. Their frequency and luminosity distributions should be a smooth extension towards higher luminosities of that of “ordinary”  $\sim$ stellar mass systems, emerging from the standard stellar evolution sequence. Although some of the ULXs might be indeed rare and exotic objects, it appears that majority of them cannot be a completely different type of the source population, but, rather, represent the high mass, high  $\dot{M}$  tail of the HMXB population.

The luminosity of ULXs in the nearby galaxies has a maximum value of the order of  $\lg(L_X) \sim 40.5$ . The fact that the galaxies from the Hubble Deep Field North obey the same  $L_X$ –SFR relation (Fig.4), implies, that the ULXs at the redshift of  $z \sim 0.2 - 1.3$  were not significantly more luminous, than those observed in the nearby galaxies.

## 4.3. Intermediate mass black holes

The hypothetical intermediate mass black holes, probably reaching masses of  $\sim 10^{2-5} M_{\odot}$ , might be produced, e.g. via black hole merges in the dense stellar clusters, and can be associated with extremely high star formation rates. To accrete efficiently, they should form close binary systems with normal stars or be located in dense molecular clouds. It is natural to expect, that such objects are significantly less frequent than  $\sim$ stellar mass black holes. The transition from the  $\sim$ stellar mass BH HMXB to intermediate mass BHs should manifest itself as a step in the luminosity distribution of compact sources (Fig.5, left panel). If the cut-off in the HMXB luminosity function, observed at  $\lg(L_{\text{cut}}) \sim 40.5$

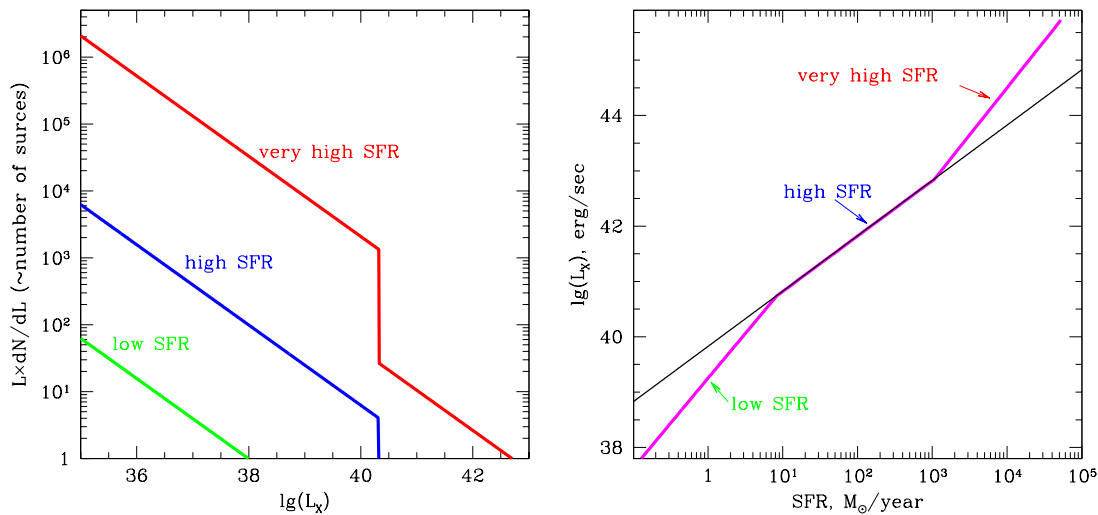


Figure 5. Illustration of the effect of hypothetical intermediate mass black holes on the  $L_X$ –SFR relation. *Left*: The luminosity function of compact sources at different levels of star formation rate. *Right*: Corresponding  $L_X$ –SFR relation. The thin straight line shows the linear relation.

corresponds to the maximum possible luminosity of  $\sim$ stellar mass black holes and if at  $L > L_{\text{cut}}$  a population of hypothetical intermediate mass BHs emerges, it should lead to a drastic change in the slope of the  $L_X$ –SFR relation at extreme values of SFR [6] (Fig.5, right panel). Therefore, observations of distant star forming galaxies with very high SFR might be an easy way to probe the population of intermediate mass black holes.

## REFERENCES

1. Brandt W.N. et al., 2001, AJ, 122, 2810
2. Colbert E.J.M. & Mushotzky R.F., 1999, ApJ, 519, 89
3. Fabbiano G., 1989, ARA&A, 27, 87
4. Gilfanov M., 2003, submitted to MNRAS (astro-ph/0309454)
5. Gilfanov M., Grimm H.-J. & Sunyaev R., 2003, submitted to MNRAS (astro-ph/0301331)
6. Gilfanov M., Grimm H.-J. & Sunyaev R., 2003, in preparation
7. Grimm H.-J., Gilfanov M. and Sunyaev R., 2002, A&A, 391, 923
8. Grimm H.-J., Gilfanov M. & Sunyaev R., 2003, MNRAS, 339, 793
9. Kennicutt R.C., 1998, ARA&A 36, 189
10. Ranalli P., Comastri A. & Seti G., 2003, A&A, 399, 39
11. Sunyaev R.A., Tinsley B.M. and Meier D.M., 1978, Comment. Astrophys., 7, 183
12. Verbunt F. & van den Heuvel E.P.J., 1995, in: X-ray Binaries, Eds: W.Lewin, J.van Paradijs & E.van den Heuvel, Cambridge Univ.Press, p.457